Accepted Preprint first posted on 21 November 2016 as Manuscript JME-16-0184

Filamin A is reduced and contributes to the CASR sensitivity in human parathyroid tumors.

Mingione Alessandra[1], Verdelli Chiara[2], Ferrero Stefano[3], Vaira Valentina[4], Guarnieri Vito[5], Scillitani Alfredo [6], Vicentini Leonardo[7], Balza Gianni[8], Beretta Edoardo[9], Terranegra Annalisa[10], Vezzoli Giuseppe[11], Soldati Laura[1*], Corbetta Sabrina[12*].

*Soldati Laura and Corbetta Sabrina are both corresponding authors.

[1]Department of Health Sciences, University of Milan, Milan, Italy; mingione.alessandra@gmail.com; laura.soldati@unimi.it

[2]Laboratory of Experimental Endocrinology, IRCCS Istituto Ortopedico Galeazzi, Milan, Italy; chiara.verdelli@libero.it

[3]Division of Pathology, Department of Biomedical, Surgical and Dental Sciences, University of Milan, Fondazione IRCCS Ca' Granda Ospedale Maggiore Policlinico, Milan, Italy; stefano.ferrero@unimi.it

[4]Division of Pathology, Department of and Transplantation, University of Milan, Fondazione IRCCS Ca' Granda Ospedale Maggiore Policlinico and Istituto Nazionale Genetica Molecolare (INGM) Romeo ed Enrica Invernizzi, Milan, Italy; valentina.vaira@unimi.it

[5]Medical Genetics, IRCCS Hospital Casa Sollievo della Sofferenza, San Giovanni Rotondo (FG), Italy; vitoguarnieri@yahoo.it

[6]Endocrine Unit, IRCCS Hospital Casa Sollievo della Sofferenza, San Giovanni Rotondo (FG), Italy; alscill@tin.it

[7]Endocrine Surgery, IRCCS Fondazione Ca' Granda Ospedale Maggiore Policlinico, Milan, Italy; viceleo@hotmail.com

[8]Internal Medicine Unit, A.O.Alessandro Manzoni, Lecco, Italy; g.balza@ospedale.lecco.it

[9]Endocrine Surgery, IRCCS Ospedale San Raffaele, Milan, Italy; beretta.edoardo@hsr.it

[10]Sidra Medical and Research Center, Doha, Qatar; aterranegra@sidra.org

[11]Nephrology and Dialysis Unit, IRCCS Ospedale San Raffaele, Milan, Italy; vezzoli.giuseppe@hsr.it

[12]Endocrinology Service, Department of Biomedical Sciences for Health, University of Milan, IRCCS Istituto Ortopedico Galeazzi, Milan, Italy; sabrina.corbetta@unimi.it

Short title: Filamin A in human parathyroid tumors

Key words: filamin A, calcium-sensing receptor, parathyroid tumors, primary hyperparathyroidism

Correspondence to:

Sabrina Corbetta, MD, PhD
Associate Professor of Endocrinology
Head of Endocrinology and Experimental Endocrinology Laboratory
Department of Biomedical Sciences for Health
University of Milan
IRCCS Istituto Ortopedico Galeazzi
Via R.Galeazzi 4, 20161 Milan, Italy
Phone +39 02 50319976, +39 02 66214647
Email sabrina.corbetta@unimi.it
And
Laura Soldati
Department of Health Sciences
University of Milan,
Via di Rudinì 8, 20142 Milan, Italy
Phone +39 02 50323035
Email laura.soldati@unimi.it

Abstract (250 words)

Parathyroid tumors display reduced sensitivity to extracellular calcium ($[Ca^{2+}]_o$). $[Ca^{2+}]_o$ activates calcium-sensing receptor (CASR), which interacts with the scaffold protein filamin A (FLNA). The study aimed to investigate: 1) the FLNA expression in human parathyroid tumors, 2) its effects on the *CASR* mRNA and protein expression, and 3) on ERK signaling activation, 4) the effect of the carboxy-terminal CASR variants and 5) of the treatment with the CASR agonist R568 on FLNA-mediated ERK phosphorylation in HEK293 cells.

Full-length FLNA immunostaining was variably reduced in parathyroid tumors. Immunofluorescence showed that FLNA localized in membrane and cytoplasm and co-localized with CASR in parathyroid adenomas (PAds)-derived cells. Cleaved C-terminus FLNA fragment could also be detected in PAds nuclear protein fractions. In HEK293 cells transfected with 990R-CASR or 990G-CASR variants, silencing of endogenous *FLNA* reduced *CASR* mRNA levels and total and membrane-associated CASR proteins. In agreement, *FLNA* mRNA levels positively correlated with *CASR* expression in a series of 74 PAds; however, any significant correlation with primary hyperparathyroidism severity could be detected and *FLNA* transcript levels did not differ between PAds harboring 990R or 990G *CASR* variants. R568 treatment was efficient in restoring 990R-CASR and 990G-CASR sensitivity to $[Ca^{2+}]_o$ in absence of FLNA.

In conclusion, FLNA is down-regulated in parathyroid tumors and parallels the *CASR* expression levels. Loss of FLNA reduces *CASR* mRNA and protein expression levels and the CASR-induced ERK phosphorylation. FLNA is involved in receptor expression, membrane localization and ERK signaling activation of both 990R and 990G CASR variants.

Introduction

Tumors of the parathyroid glands display reduced sensitivity to extracellular calcium ($[Ca^{2+}]_o$) resulting in failure in inhibiting parathormone (PTH) synthesis and release. Overall, derangements in calcium sensing result in increased parathyroid cell proliferation. The parathyroid cell sensitivity to $[Ca^{2+}]_o$ is mediated by the calcium-sensing receptor (CASR). CASR is a G-protein coupled membrane receptor interacting with different intracellular pathways (Breitwieser 2013; Conigrave & Ward 2013): active CASR dimers increase inositol-triphosphate and intracellular calcium concentrations, activate protein kinase C and intracellular calcium oscillations, and stimulate mitogen activated protein kinase (MAPK) cascade through p44/42 extracellular signaling-regulated kinase (ERK) phosphorylation (Breitwieser & Gama 2001; Corbetta *et al.* 2002; Chakravarti *et al.* 2012). CASR activates intracellular signaling through direct interaction with Gq/11 protein and the cytoskeletal scaffold protein filamin A (Awata *et al.* 2001; Hjalm *et al.* 2001).

Parathyroid tumors are characterized by variable degrees of insensitivity to $[Ca^{2+}]_o$, sustained by deregulation of key molecular components of CASR-coupled intracellular signaling: *CASR* mRNA and protein expression is down-regulated (Corbetta *et al.* 2000; Varshney *et al.* 2013a); the major 990R allele of the *CASR* gene is associated with higher serum PTH levels (Corbetta *et al.* 2006) in hyperparathyroid patients and with *in vitro* lower responsiveness to $[Ca^{2+}]_o$ than the minor *CASR* 990G allele (Terranegra *et al.* 2010); Gq/11 protein expression is reduced (Corbetta *et al.* 2000); CASR-stimulated p44/42 ERK activity is blunted (Corbetta *et al.* 2002).

Filamin A (FLNA) is a 280 kDa protein that contains N-terminal actin-binding domain and consists of 24 repeated domains of approximately 96 amino acids each. FLNA is a scaffolding molecule facilitating protein interaction. The C-terminal domains 14 and 15 of FLNA interact with the carboxyl-terminal portion of CASR (Awata *et al.* 2001; Hjalm *et al.* 2001). This interaction stabilizes CASR in membrane and reduces its degradation, thereby facilitating the MAPK signaling

(Zhang & Breitwieser 2005). In adult cells, FLNA regulates cell cycle: suppression of FLNA leads to prolongation of the cell cycle, mainly in the M phase, and increases phosphorylation of cyclin-dependent kinase 1 (Lian *et al.* 2012). Moreover, FLNA plays a significant role in cancer development and progression: a number of human cancers overexpress FLNA. By contrast, in human prolactin-secreting pituitary adenomas resistant to dopamine treatment, a tumor model close to human parathyroid tumors, FLNA expression is diminished and involved in dopamine resistance (Peverelli *et al.* 2012).

Data about FLNA in parathyroid cells are from neonatal bovine parathyroid glands, whose dispersed cells express endogenously FLNA at confocal immunofluorescence microscopy: FLNA exhibits the highest density within the cytoplasm and colocalizes with endogenous CASR proteins (Hjalm *et al.* 2001). To our knowledge, data about FLNA expression in human parathyroid cells from normal or tumor glands are still lacking.

In the present study, we investigated: 1) the FLNA expression in parathyroid adenomas and carcinomas samples compared to normal glands from normocalcemic subjects; 2) the effects of FLNA loss on CASR expression, 3) on CASR-activated ERK signaling and 4) in presence of the CASR agonist R568 in HEK293 cells transiently transfected with CASR; 5) whether the 990G-CASR variant expression and function were differently affected by FLNA loss with respect to the 990R variant.

Methods

Sample collection

Formalin-fixed paraffin-embedded sections from 4 normal parathyroid glands incidentally removed during thyroid surgery of normocalcemic patients, 17 parathyroid tumors (10 typical

parathyroid adenomas and 7 parathyroid carcinomas) from patients with primary hyperparathyroidism (PHPT) were collected and analyzed by immunohistochemistry. Fresh tissue samples from 3 parathyroid adenomas (PAds) were collected, fragmented and the dispersed cells were cultured for immunofluorescence experiments.

Immunohistochemistry (IHC)

Archival parathyroid normal and tumor samples (6 normal parathyroid glands incidentally removed from normocalcemic patients during surgery for thyroid diseases, 10 sporadic benign PAds and 7 parathyroid carcinomas (PCas) from patients with PHPT were used for immunhistochemistry after tissues morphology was assessed by haematoxylin and eosin staining. Histological diagnosis of parathyroid carcinoma was established according to WHO published guidelines (Bondeson *et al.* 2004). Briefly, IHC was performed using an anti-human full-length FLNA antibody (1:200; Abnova Corporation, Taipei City, Taiwan) as previously described (Peverelli *et al.* 2012). Slides with absence of the primary antibody were included as negative controls. Percentage of positive cells was calculated considering at least 400 cells in the main representative high-power field, as previously described (Lania *et al.* 2004); blinded scoring of the cells was performed by an experienced pathologist (S.F.).

Immunofluorescence (IF)

Human PAds-derived cells (n=3) cultured for 48 hours, and subconfluent HEK293 cells were fixed in 4% paraformaldehyde, permeabilized in 0.1% Triton X-100, and blocked in 1% BSA-PBS for 2 hours. Then, cells were incubated with primary antibodies against human full length FLNA (mouse monoclonal H00002316-M01; Abnova Corp., Taipei, Taiwan) and human CASR (rabbit polyclonal PA1-934; Affinity Bioreagents, Golden, CO, USA), overnight at 4°C, washed thrice in PBS and followed by incubation with secondary antibodies conjugated with FITC or DyLight549 (1:100; Jackson Immuno Research, Milan, Italy). Nuclei were stained with Hoechst

33342 (1:500 dilution). For negative controls, PBS was used instead of primary antibodies to exclude unspecific binding of secondary antibody. Images were captured using a fluorescent confocal microscope (TCS SP2, Leica, Milan, Italy) and a digital camera.

Nuclear cleaved FLNA fragment expression in parathyroid tissues

Cells were homogenized using a Nuclear Extract kit (Active Motif, Carlsbad CA USA) following the manufacturer's instructions in order to obtain both citoplasmic and nuclear protein fractions. The kit provide protease and phosphatase inhibitors cocktail for the cell lysis and protein extraction procedures. Samples (40 μg proteins) were denatured with loading dye and β-mercaptoethanol for 10 min at 95°C. Proteins were separated on 10% w/v SDS-PAGE and antigen were revealed by a primary antibody that recognized the C-terminal (90-100kDa) calpain cleavage fragment of Filamin A (Millipore, Darmstadt, Germany). Histone H3 was used as internal control (Abcam, Cambridge, UK). Specific protein bands were detected using SuperSignal West Pico enhanced chemiluminescence system (Pierce, Rockford, IL, USA).

Quantitative Real-Time PCR

Total RNA was extracted from frozen human PAds samples using Trizol Reagent (ThermoFischer Scientific) following manufacturer's instructions. One microg of RNA was digested with DNAse I (ThermoFischer Scientific) to remove genomic DNA contamination and reverse-transcribed using the iScript cDNA Synthesis Kit (BioRad, Segrate, Milan, Italy). *CASR* and *FLNA* expression levels were estimated by quantitative real-time PCR using specific primers: *CASR* gene (Forward: 5'-ATGCCAAGAAGGGAGAAAGACTCTT-3'; Reverse: 5'-TCAGGACACTCCACACACTCAAAG-3'); *FLNA* gene (Forward: 5'-CAGTGCTATGGGCCTGGTAT-3'; Reverse: 5-'CCACTTTGTACATGCCATCG-3'); housekeeping *GAPDH* gene (Forward: 5'-CTCATGA-CCACAGTCCATGCCATC-3' and Reverse: 5'-CATGCCAGTGAGCTTCCCGTT-3'). Real-time PCR was performed with 7500 Fast Real-

Time PCR Systems (Applied Biosystems, Life Technologies) with 100 ng of cDNA as template and SYBR Premix Ex TaqTM II (Takara Bio Inc, Japan). Specific temperature of primers annealing were 57°C for *CASR* gene, 65°C for *FLNA* gene or 60°C for *GAPDH*. Mean cycle threshold values of triplicate samples were used for analysis. Data were analyzed by 7500 Fast System SDS Software. *CASR* and *FLNA* mRNA quantities were normalized using the housekeeping *GAPDH* expression levels and data were expressed as *CASR*/*GAPDH* and *FLNA*/*GAPDH* mRNA ratios.

Culture of parathyroid adenomas (PAds)-derived and Human Embryonic Kidney (HEK293) cells

Samples from human parathyroid adenomas (PAds) were cut into fragments less than 1 mm^3, washed with PBS and partially digested with 2 mg/ml collagenase type I (Worthington, Lakewood, NJ, USA). After digestion, tissues fragments were filtered with a cell strainer (100 μm Nylon, BD Falcon, Milan, Italy). Cells derived from human PAds and Human Embryonic Kidney (HEK293) cells were routinely grown in DMEM medium, supplemented with 10% FBS, 2 mM L-glutamine and 1% penicillin/streptomycin (all from Gibco-Invitrogen, ThermoFischer Scientific, Wlatham, MA, USA) under standard culture conditions (5% CO_2, 37°C).

CASR gene transfection and FLNA silencing

HEK293 cells were plated in MW6 plates at a density of 10^5 cells/well in complete medium. When cells reached 70-90% confluence, they were simultaneously silenced for *FLNA*, with predesigned small interfering RNA (siRNA) (Stealth RNAi HSS103734, Invitrogen), and transiently transfected with plasmid encoding for wild-type *CASR* (990R-*CASR*), obtained by site-directed mutagenesis as previously described (Terranegra *et al.* 2010) or 990G-*CASR*, kindly provided by Dr Jianxin Hu (NIH, Bethesda, MD, USA). Transfection, silencing and co-transfection was performed with 10, 5 and 12 μl Lipofectamine 2000 (Invitrogen) respectively, 4 μg CASR plasmid and 500 pmol of FLNA siRNA in OptiMEM serum-free medium (Invitrogen) for each well. To obtain the best efficiency of *FLNA* silencing, three different human *FLNA* siRNA were tested. Preliminary experiments to determine the optimal concentration of siRNA and the *FLNA*

204 silencing kinetics were performed. As negative control in each experiment, medium GC duplex
205 stealth RNAi negative control duplex human (control-siRNA) was used as indicated by manufacture
206 instructions (Invitrogen). The growth medium was changed to starvation medium (serum-free
207 medium supplemented with 0.2% BSA and 1% penicillin/streptomycin) 24 hours after co-
208 transfection. Gene expression and activity were tested 72 hours after transfection.

209 *Total and membrane CASR and FLNA proteins quantifications*

210 HEK293 cells, plated in MW6 plates, were trypsinized and the pellets were lysed with ice-
211 cold lysis buffer (150 mM NaCl, 10 mM TRIS-HCl pH 7.2, 0.1% SDS, 1% Triton X-100, 1%
212 deoxycholate, 5 mM EDTA, 1 mM PMSF, 10 mM benzamidine, 2μg/ml leupeptin, 0.1 mM Na-
213 Orthovanadate). The lysates were centrifuged and the surnatants were recollected to quantify
214 proteins by BCA protein assay kit (Pierce). The membrane proteins extraction was performed with
215 Mem-Per plus Kit by manufacture instructions (ThermoFischer Scientific, Life Technologies Italia,
216 Monza, MB, Italy). All samples (10 μg proteins/well) were denatured with loading dye buffer and
217 β-mercaptoethanol for 10 min at 95°C to obtain proteins for FLNA and ERK analysis, or with
218 denaturing buffer: 7M Urea, 2 M Thiourea, 65 mM DTT, 5x Laemmli sample buffer (final
219 concentration 2% SDS) for 30 min at room temperature for the analysis of the CASR dimeric (250
220 kDa) and monomeric (130-150 kDa) receptor isoforms. Iodoacetamide (130 mM) was added to
221 block DTT for 30 min at room temperature. Proteins were separated by 8% w/v SDS-PAGE, then
222 electrotransferred to PVDF membrane. The blots were blocked in a blocking solution (5% milk in
223 TBST or 5% BSA in TBST) and then incubated overnight at 4°C with different antibodies: 1:5000
224 dilution monoclonal CASR antibody (Affinity Bioreagents, Golden, CO, USA), 1:10000 dilution
225 monoclonal anti-GAPDH antibody (Abnova Corporation, Taipei, Taiwan), 1:1000 dilution
226 polyclonal anti-β-actin antibody (Sigma Chemicals, St Louis, MO, USA) and 1:1000 dilution anti-
227 Na/K-ATPase antibody (Cell Signaling, Danvers, MA, USA), for 2 hours at room temperature. The

228 FLNA expression levels were assessed in each experiment with 1:5000 dilution monoclonal full-
229 length FLNA antibody (Abnova Corporation). Membranes were incubated in the blocking solution
230 with secondary horseradish peroxidase-coupled anti-mouse or anti-rabbit IgG (Jackson
231 ImmunoResearch Laboratories, Suffolk, UK). Specific protein bands were detected using
232 SuperSignal West Pico enhanced chemiluminescence system (Pierce, Rockford, IL, USA).
233 Experiments were repeated at least thrice. The band intensities, corresponding to the levels of
234 protein expression, were measured by Image J software.

235 *Phosphorylated ERK1/2 quantification*

236 Serum-starved transfected HEK293 cells were stimulated with increasing concentrations of calcium
237 chloride (CaCl2; 0.5, 1.0, 3.0 and 5.0 mM) with or in absence of the calcimimetic R568 (0.01 μM;
238 kindly provided by Amgen Inc., Thousand Oaks, CA, USA) for 10 min at 37°C in saline solution
239 PSS (NaCl 125 mM, KCl 4 mM, HEPES 20 mM, D-Glucose 0.1%, NaH2PO4 0.8 mM, MgCl2 1
240 mM, pH 7.45). Incubation was stopped by placing the cells on ice. The PSS was removed and cells
241 were treated with 50 μl ice-cold lysis buffer as described above, supplemented with complete
242 phosphatase inhibitor cocktail (Roche Diagnostics Spa, Monza, MB, Italy). Samples (20 μg
243 proteins/well) were denatured with loading dye and β-mercaptoethanol for 10 min at 95°C. Proteins
244 were separated on 10% w/v SDS-PAGE and analysis of ERK1/2 activation was performed by
245 western blot with 1:1000 and 1:2000 dilution polyclonal anti-p44/42 ERK and anti-phospho-p44/42
246 ERK antibodies, respectively (Cell Signaling Technology, Beverly, MA, USA). Specific protein
247 bands were detected by a chemiluminescent method as described above for CASR and FLNA
248 proteins quantification. Experiments were repeated at least thrice.

249 *Genotyping*

250 Genomic DNA was extracted from 74 frozen human PAds tissues samples using Trizol
251 reagent (Invitrogen) following manufacture's instructions. *CASR* R990G SNP genotyping was

performed by a specific Taqman® SNP genotyping assay (C_7504854_20, Life Technologies Ltd, Inchinnan, UK) with the Applied Biosystems® 7500 Fast Real-Time PCR Systems. Amplification was performed in 8 µl final volume with 20 ng of genomic DNA at the following conditions: 95°C for 20 sec, and 40 cycles each of 95°C for 3 sec and 60°C for 30 sec. SNP variation was assessed by means of the allelic discrimination assay employing the Applied Biosystems Software Package SDS 2.1.

PHPT patients

We collected the clinical and biochemical data of the 74 patients with primary hyperparathyroidism (PHPT)(57 females, 17 males, age 59.7±14.2 years), whose surgically removed PAds were analyzed. PHPT was diagnosed when hypercalcemia (serum calcium>10.2 mg/dL and/or ionized calcium>1.30 mmol/L) and elevated or inappropriately normal serum PTH level occurred. Exclusion criteria were diagnosis of familial hypocalciuric hypercalcemia [detection of calcium-to-creatinine clearance ratio > 0.01 following vitamin D deficiency correction (Marcocci *et al.* 2015)], previously established diagnosis of chronic kidney disease, hyperthyroidism, pregnancy, glucocorticoids, bisphosphonates, diuretics and calcimimetic treatments. All patients were Caucasians. Patients underwent clinical and laboratory evaluation, including: 1) personal and family medical history; 2) physical examination including arterial blood pressure, weight and height measurement; 3) fasting biochemical evaluation including total and ionized calcium, phosphate, intact PTH, 25hydroxyvitaminD3, creatinine; a 24 hours urine collection was obtained from all patients for urinary calcium and phosphate excretion; 4) imaging evaluation including lumbar and femoral dual-energy X-ray absorptiometry (DEXA), vertebral spine X-ray and ultrasound kidney examination. Osteoporosis was diagnosed in 50% and kidney stones in 30% of PHPT patients. Biochemical and hormonal parameters were assayed by routine methods. All participants gave their

informed consent after full explanation of the purpose and nature of all used procedures; the protocol study was approved by the local ethics committee.

Statistical analysis

Results are expressed as mean±standard error of the mean (SEM) or median and range interquartile. Analysis of variance was performed by ANOVA or Wilcoxon rank-sum tests. Correlation between *FLNA* and *CASR* expression levels in PAds was analyzed by linear regression analysis. Differences between two groups were tested by Student's *t*-test or Mann Whitney test. A p-value < 0.05 was considered statistically significant.

Results

FLNA protein expression in human normal and tumor parathyroids

In normal parathyroid glands (n=6), most epithelial parathyroid cells showed intense staining for full-length FLNA in the cytoplasm and at membrane level (Fig. 1, *panel A*, a). Endothelial cells lining the vessels showed intense staining for FLNA [arrows in Figure 1, *panel A,* a-c] and were considered as internal positive controls. A pattern of staining similar to that in normal parathyroid glands was detected in sporadic parathyroid adenomas samples (PAds, n=10), though the amount of FLNA-expressing cells was variably reduced among the samples (Fig. 1, *panel A*, b-c) ranging from 50% to 10% of tumor parathyroid epithelial cells. Remarkably, the FLNA-expressing cells were <10% or absent in parathyroid carcinomas (PCas, n=7) (Fig. 1, *panel A*, d). Therefore, a subset of PAds and the most PCas showed a variable loss of FLNA-expressing cells (Fig. 1, *panel B*). By immunofluorescence on PAds-derived cultured single cells, full-length FLNA was detected at membrane level and in the cytoplasm of a subset of tumor parathyroid cells, where it co-localized with CASR with a membrane and peripheral cytoplasmic distribution (Fig. 1, *panel C*). Indeed, immunoblotting fractioned proteins from HEK293 cells and PAds, using a primary

antibody against the C-terminal calpain cleaved fragment of FLNA, detected a specific band of 100 kDa in the nuclear protein fractions. An additional band of 270 kDa corresponding to the full-length FLNA, was also visualized in all samples (Fig. 1, *panel D*); the nuclear accumulation of full-length FLNA, though detected by IHC in some tumor cells (data not shown), may be related to the sensitivity of the immunoblotting on fractioned proteins.

Effect of FLNA gene silencing on CASR expression levels

The effect of FLNA loss on CASR expression was investigated in 990R-CASR-transiently transfected HEK293 cells silenced for FLNA by siRNA technique. As shown in Fig. 2, *panel A*, in HEK293 cells, 72 hours-FLNA silencing consistently decreased endogenous FLNA protein expression (about 70-80%), compared to control siRNA transfected cells. The siRNA efficiency was not affected by cotransfection of the CASR plasmids (Fig. 2, *panel A*).

Loss of FLNA significantly reduced the total and membrane 990R-CASR protein levels (Fig. 2, *panels B* and *C*). Cotransfection of the 990R-CASR plasmid and control siRNA did not affect the 990R-CASR expression levels both in the total and in the membrane protein fractions, which were similar to those detected in HEK293 cells transfected with the 990R-CASR plasmid alone (Fig. 2, *panels B* and *C*).

FLNA and CASR mRNA expression levels in PAds

Loss of FLNA-induced CASR protein reduction might be due to reduced receptor stabilization with consequent increased degradation and/or by inhibition of *CASR* gene expression. The FLNA full-length and cleaved fragments can regulate gene expression directly or indirectly through interaction with a number of intracellular pathways (Savoy & Ghosh 2013). We observed that FLNA silencing also reduced *CASR* mRNA levels in 990R-CASR-HEK293 cells (Fig. 3, *panel A*). HEK293 cells do not express endogenous *CASR* gene and protein and the 990R-CASR-HEK293

cell model was generated by transfecting a *CASR* plasmid lacking the endogenous regulatory region. Therefore, loss of FLNA-induced *CASR* inhibition could not be a direct nuclear effect.

We further investigated *FLNA* and *CASR* mRNA expression levels in tissue samples from 74 sporadic PAds surgically removed from patients with a clinical and hormonal diagnosis of PHPT. *FLNA* and *CASR* mRNA levels, reported as a ratio with *GAPDH* mRNA, were highly variable among PAds samples and *CASR* mRNA levels positively correlated with *FLNA* mRNA levels (r^2=0.223 P<0.0001) (Fig. 3, *panel B*), suggesting a potential modulation of the CASR gene transcript by FLNA. Nonetheless, *FLNA* and *CASR* mRNA levels of PAds did not show any significant correlation with the PHPT severity (Table 1): *FLNA* and *CASR* mRNA levels of PAds associated with severe PHPT, defined as clinical diagnosis of kidney stones and/or osteoporosis and/or osteoporotic fractures and/or serum calcium > 1 mg/dl above the upper limit of the normal range, were similar to those detected in PAds associated with mild PHPT (Marcocci *et al.* 2015).

However, CASR and FLNA protein expression levels, detected by western blot analysis, did not show significant correlation (Fig. 3A and 3B): though there were tumors (PAd1 and PAd6) with low FLNA levels and low CASR levels or high FLNA levels and high CASR levels (PAd2), other tumors (PAd 3 and PAd4) had low FLNA levels and consistent CASR expression levels or high FLNA levels and low CASR levels (PAd5).

Effect of the 990G CASR allele on FLNA and CASR mRNA expression

Genotyping for the *CASR* 990 single nucleotide variants of the PAds samples identified 68 tumors harboring the major allele 990R and 6 tumors harboring the minor allele 990G of the *CASR* gene. PAds harboring the 990G CASR variant were associated with mean serum intact PTH levels lower than those in PAds harboring the 990R variant (171.0±24.9 vs 328.1±44.0 pg/ml, P=0.003), while mean serum albumin-corrected calcium levels were similar (11.3±0.4 vs 11.6±0.1 mg/dl; P=0.76). No significant difference could be detected in the PAds harboring the 990R compared with PAds harboring the 990G variants in the median expression levels of the *FLNA* (median, range

interquartile: 0.08, 0.04-0.15 vs 0.09, 0.06-0.31; P=0.33; Fig. 4, *panel C*) and *CASR* genes (median, range interquartile: 0.68, 0.43-0.96 vs 0.84, 0.56-2.98; P=0.14; Fig. 4, *panel D*).

Effect of FLNA gene silencing on the CASR-stimulated p44/42 ERK phosphorylation

To evaluate the effect of the loss of FLNA expression on the CASR-activated signaling, we measured the levels of phosphorylated p44/42 ERK in 990R-CASR cells after FLNA silencing. After 72 hours-incubation with FLNA siRNA or control siRNA, 990R-CASR was activated by increasing extracellular calcium concentrations ($[Ca^{2+}]_o$), from 0.5 to 1.0, 3.0, and 5.0 mM, as shown in Fig. 5, *panel A*. Loss of FLNA expression in 990R-CASR HEK293 cells did not significantly alter ERK phosphorylation levels at 0.5 and 1.0 mM $[Ca^{2+}]_o$, while at 3.0 and 5.0 mM $[Ca^{2+}]_o$ it significantly decreased the 990R-CASR activation induced phospho-ERK levels compared to those detected in 990R-CASR HEK293 cells transfected with the control siRNA (0.75±0.06 *vs* 0.92±0.08; *P*=0.006 at 3.0 mM $[Ca^{2+}]_o$; 0.71±0.24 *vs* 1.21±0.38; *P*=0.02 at 5.0 mM $[Ca^{2+}]_o$)(Fig. 5, *panel A*). The incubation with the potent calcimimetic R568 0.01 μM blunted the effect of FLNA loss on the 990R-CASR-induced phosphorylation of ERK at any $[Ca^{2+}]_o$ (Fig. 5, *panel B*).

Effects of the 990G CASR allele on FLNA-modulated CASR protein expression and CASR-mediated ERK phosphorylation

In HEK293 cells co-transfected with either 990R-CASR and 990G-CASR and siRNA control, we observed that the amount of 990G-CASR in the membrane protein fraction was significantly higher than that of 990R-CASR (5.3±0.25 vs 4.4±0.1, P=0.03) (Fig. 2, *panel C*). Loss of FLNA in 990G-CASR-HEK293 cells reduced the total and membrane 990G-CASR protein levels at an extent similar to that observed in the 990R-CASR transfected HEK293 cells (Fig. 2, *panels B* and *C*). In HEK293 cells transfected with the 990G-CASR and endogenous FLNA, 990G-

CASR activation by increasing $[Ca^{2+}]_o$ stimulated ERK phosphorylation at higher levels than that observed in 990R-CASR-expressing cells, which gained the statistical significance at 5.0 mM $[Ca^{2+}]_o$ (2.80±0.68 vs 1.21±0.38; P=0.02), in agreement with previous report (Terranegra *et al.* 2010)(Fig. 5, *panel A*). Loss of FLNA by treatment with siRNA reduced 990G-CASR-induced phospho-ERK levels with a significant difference at 5.0 mM $[Ca^{2+}]_o$ (1.33±0.43 vs 2.80±0.68; P=0.04)(Fig. 5, *panel A*). Finally, treatment of 990G-CASR-HEK293 cells with 0.01 μM R568 blunted the effect of FLNA loss as observed in 990R-CASR-expressing cells, though, in presence of FLNA, 990G-CASR-expressing cells showed higher $[Ca^{2+}]_o$-induced phospho-ERK levels than 990R-CASR-expressing cells reaching statistically significance at 3.0 mM and 5.0 mM $[Ca^{2+}]_o$ (3.10±0.34 vs 1.94±0.38 and 3.13±0.20 vs 2.48±0.03, respectively; P=0.04) (Fig. 5, *panel B*), in agreement with previous report (Terranegra *et al.* 2010).

Discussion

In the present study, the scaffold protein filamin A (FLNA) was firstly shown to be down-regulated in human parathyroid tumors. Most cells in normal parathyroid glands expressed full-length FLNA protein in cytoplasm and in association with membrane, while FLNA-expressing cells were variably reduced in parathyroid adenomas with tumor samples displaying an immunostaining pattern similar to that in normal glands and samples with a proportion of FLNA-expressing cells less than 10%. FLNA-expressing cells were definitely reduced in all the parathyroid carcinomas samples. Loss of FLNA expression has been reported in prolactin-secreting pituitary tumors (Peverelli *et al.* 2012), where it is related to dopamine-resistance, at variance with the increased expression detected in a variety of human cancers. The role of FLNA in tumorigenesis is complex and related to its subcellular localization: as scaffold protein, FLNA interacts with receptors localized in membranes; as cytoplasmic protein, FLNA functions in various growth signaling

394 pathways, such as vascular endothelial growth factor, R-Ras and integrin signaling; as nuclear
395 active cleaved fragment, it interacts with transcription factors and nuclear receptors (Savoy &
396 Ghosh 2013). In human parathyroid tumor cells, full-length FLNA was localized in membrane and
397 in cytoplasm, similarly to what reported in bovine parathyroid cells (Hjälm *et al.* 2001); in addition,
398 cleaved FLNA fragment could be detected in the nuclear protein fractions, suggesting FLNA
399 potential involvement in multiple regulatory pathways in parathyroid tumor cells.

400 Parathyroid tumors are characterized by extracellular calcium insensitivity (Corbetta *et al.*
401 2000) and loss of CASR expression: compared with normal parathyroid glands, both *CASR* mRNA
402 and protein are down-regulated in parathyroid adenomas (Kawata *et al.* 2006; Yano *et al.* 2003),
403 carcinomas (Haven *et al.* 2004, Wittenveen *et al.* 2011) and primary and secondary hyperplasia
404 (Martin-Salvago *et al.* 2003; Latus *et al.* 2013; Varshney *et al.* 2013a). *CASR* gene mutations have
405 been rarely identified in sporadic parathyroid tumors (Frank-Raue *et al.* 2011; Guarnieri *et al.* 2010)
406 and *CASR* gene deregulation is not sustained by promoter hypermethylation (Varshney *et al.*
407 2013b). Therefore, alternative mechanisms might induce *CASR* mRNA and protein downregulation
408 in parathyroid tumor cells. It has been reported in HEK293 cells stably transfected with CASR that
409 FLNA interaction with CASR carboxyl terminal tail (Awata *et al.* 2001) is required for CASR
410 stabilization through attenuation of its degradation (Zhang & Breitwieser 2005). We tested the
411 hypothesis that down-regulation of CASR expression might be related to loss of FLNA in
412 parathyroid tumors. We performed *in vitro* studies to investigate the effect of FLNA loss on CASR
413 expression levels. Experiments were realized in HEK293 cells transiently transfected with 990R-
414 CASR because lack of suitable human parathyroid cells; a robust cell system has been developed,
415 where unspecific effects of *CASR* plasmids and *FLNA* siRNA co-transfection were ruled out. Loss
416 of FLNA significantly reduced the 990R-CASR expression levels both in the total protein pools and
417 in the membrane protein fractions, suggesting an involvement of FLNA in stabilization of 990R-

418 CASR proteins in HEK293 cells. Indeed, loss of FLNA reduced also *CASR* mRNA levels,
419 suggesting that FLNA might be active on *CASR* gene regulation, likely at post-transcriptional level
420 (Savoy *et al.* 2015). In parathyroid adenomas, *FLNA* gene expression levels positively correlated
421 with *CASR* gene expression levels, suggesting a FLNA-mediated modulation of CASR gene
422 transcription; this hypothesis is further supported by the detection in the parathyroid adenomas
423 nuclear protein fractions of cleaved FLNA fragments accumulation, which has been demonstrated
424 to directly regulate gene transcription (Savoy & Ghosh 2013). *FLNA* and/or *CASR* mRNA levels
425 did not correlate with PHPT severity, suggesting that expression of these molecules is not a major
426 determinant of the clinical phenotype associated with parathyroid tumors. Indeed, FLNA and CASR
427 protein expression levels in parathyroid adenomas showed different patterns ranging from tumors
428 with either low or high FLNA and CASR expression levels to tumors with discordant FLNA and
429 CASR expression, in line with the wide range of reduced sensitivity to extracellular calcium
430 characterizing the parathyroid tumors.

431 We further tested the hypothesis that FLNA is involved in the regulation of the CASR-
432 mediated ERK activation and, firstly, evaluated the effect of the CASR agonist R568 when FLNA
433 was reduced. FLNA interaction with CASR facilitates ERK phosphorylation (Zhang & Breitwieser
434 2005) and CASR activation increases ERK phosphorylation in human normal and tumor
435 parathyroid cells (Corbetta *et al.* 2002). In line with the previous report (Zhang & Breitwieser
436 2005), in HEK293 cells transiently transfected with 990R-CASR, *FLNA* gene silencing reduced the
437 $[Ca^{2+}]_o$-induced ERK phosphorylation. Treatment with R568 blunted the effect of FLNA loss,
438 consistent with the stabilizing effect of R568 on CASR membrane expression demonstrated in
439 previous study (Huang & Breitwieser 2007; Miedlich *et al.* 2004).

440 FLNA interacts with the CASR carboxyl terminal tail at the domain between 972 and 997
441 aminoacid residues (Awata *et al.* 2001; Hjalm *et al.* 2001). In this region, single nucleotide
442 polymorphic variants have been identified and extensively investigated for the association with

phenotype (Cetani *et al.* 2002; Mingione *et al.* 2015; Vezzoli *et al.* 2015) and with the sensitivity to CASR agonist treatment in PHPT cohorts (Vezzoli *et al.* 2015). Just inside the FLNA binding region, a non-conservative CASR polymorphism, Arg990Gly (R990G) induces a gain of function in the receptor activity (Vezzoli *et al.* 2002; Scillitani *et al.* 2004; Corbetta *et al.* 2006). We investigated whether 990G allele affects the interaction of CASR C-terminus with FLNA testing the effect of FLNA loss on CASR-induced ERK phosphorylation in HEK293 cells transfected with 990G-CASR. Similarly to what observed with 990R-CASR, FLNA loss reduced 990G-CASR mRNA in 990G-CASR transfected cells. Parathyroid tumors harboring the 990G-CASR variant do not show significant differences in *FLNA* and *CASR* mRNA expression levels compared with tumors harboring the more frequent 990R-CASR variant. Loss of FLNA also reduced 990G-CASR protein levels in both total and membrane protein fractions, though in presence of endogenous FLNA, expression of 990G-CASR in cell membrane was slightly higher than that of the 990R-CASR. Moreover, analyzing the effect of FLNA loss on 990G-CASR- and 990R-CASR-induced ERK phosphorylation, three conditions characterized by increasing sensitivity of CASR-mediated ERK activation could be identified: the less sensitive condition was determined by loss of FLNA associated with the 990R allele, while the most sensitive condition was provided by co-expression of FLNA and 990G allele. The conditions characterized by loss of FLNA associated with the 990G allele, and conserved FLNA associated with the 990R allele, displayed a variable reduced sensitivity. Nonetheless, as observed with 990R-CASR, R568 treatment was efficient in rescuing 990G-CASR sensitivity to $[Ca^{2+}]_o$ in absence of FLNA.

In conclusion, FLNA is variably down-regulated in parathyroid tumors both at mRNA and protein levels. Therefore, parathyroid tumor cells are characterized by receptor and post-receptor defects, namely loss of CASR (Martin-Salvago *et al.* 2003; Yano *et al.* 2003; Haven *et al.* 2004; Kawata *et al.* 2006; Wittenween *et al.* 2011; Latus *et al.* 2013; Varshney *et al.* 2013a), Gq/11

protein (Corbetta *et al.* 2000) and FLNA. Data about loss of FLNA in 990R-CASR-transfected HEK293 cells confirmed previously reported results: reduction of CASR protein and of CASR-induced ERK phosphorylation. We further extended investigation to the FLNA effect on *CASR* mRNA expression, finding that it is affected and therefore suggesting an additional FLNA-related deregulation, also supported by cleaved FLNA nuclear localization. Though the 990G allele was associated with increased sensitivity to $[Ca^{2+}]_o$, FLNA is required for receptor protein expression and ERK signaling activation. Treatment with R568 agonist is effective in presence of different CASR and FLNA deregulated conditions.

Admittedly, our conclusions were limited by the fact that functional experiments were performed in HEK293 cells and could not be replicated in human normal or tumor parathyroid cells. It should also be considered that FLNA has been reported to interact with over 90 proteins, which indicates the numerous pathways that FLNA can affect (Stossel *et al.* 2001). Therefore, in parathyroid tumors with loss of FLNA, intracellular pathways other than ERK signaling might be impaired and contribute to the tumor phenotype.

List of abbreviations

FLNA, filamin A

CASR, calcium-sensing receptor

PAds, parathyroid adenomas

PCas, parathyroid carcinomas

PaNs, normal parathyroid glands

PHPT, primary hyperparathyroidism

ERK, extracellular-signal-regulated kinase

PTH, parathormone

HEK-293 cells, human embryonic kidney-293 cells

GAPDH, glyceraldehyde-3-phosphate dehydrogenase

ERK, extracellular signal-regulated kinase

Acknowledgement

The study was supported by Amgen, USA, IRCCS Policlinico San Donato and IRCCS Istituto Ortopedico Galeazzi Ricerca Corrente (L4080) funds.

Conflict of interest

The Authors declare that they have no competing interests, with the exception of Laura Soldati who received funding from Amgen, USA.

Authors' Contribution Statement

MA carried out the experiments in HEK293 cells and CASR genotyping; VC performed immunofluorescence on PAds-derived cells; FS and VV carried out immunhistochemistry for FLNA on human parathyroid sections; GV performed RNA extraction from human parathyroid tumors and real-time PCR gene quantification; SA collected clinical data from PHPT patients; VL, BG, and BE collected fresh parathyroid tumor biopsies during surgery for PHPT; TA conceived experimental design in HEK293 cells and supervised MA; VG revised data on CASR genotyping; SL and SC conceived the project, collected and reviewed experimental data, discussed the results and wrote the manuscript. All Authors read and approved the final manuscript.

510

511

512

References

Awata H, Huang C, Handlogten ME & Miller RT 2001 Interaction of the calcium-sensing receptor and filamin, a potential scaffolding protein. *The Journal of Biological Chemistry* **276** 34871-34879.

Bondeson L, Grimelius L, De Lellis RA, Lloyd R, Akerstrom G, Larsson C, Arnold A, Eng C, Shane E & Bilezikian JP 2004 Parathyroid carcinoma. In *Pathology and Genetics. Tumors of Endocrine Organs*. *WHO Classification of Tumors*, pp 128-132. Eds RA DeLelli, RV Lloyd, PU Heltz & C Eng. Lyon: IARC Press.

Breitwieser GE & Gama L 2001 Calcium-sensing receptor activation induces intracellular calcium oscillations. *American Journal of Physiology. Cell Physiology* **280** C1412-C1421.

Breitwieser GE 2013 The calcium sensing receptor life cycle: trafficking, cell surface expression, and degradation. *Best Practice & Research. Clinical Endocrinology & Metabolism* **27** 303-313.

Cetani F, Borsari S, Vignali E, Pardi E, Picone A, Cianferotti L, Rossi G, Miccoli P, Pinchera A & Marcocci C 2002 Calcium-sensing receptor gene polymorphisms in primary hyperparathyroidism. *Journal of Endocrinological Investigation* **25** 614-619.

Chakravarti B, Chattopadhyay N, Brown EM 2012 Signaling through the extracellular calcium-sensing receptor. *Advances in Experimental Medicine and Biology* **740** 103-142.

Conigrave AD & Ward DT 2013 Calcium-sensing receptor (CaSR): pharmacological properties and signaling pathways. *Best Practice & Research. Clinical Endocrinology & Metabolism* **27** 315-331.

Corbetta S, Mantovani G, Lania A, Borgato S, Vicentini L, Beretta E, Faglia G, Di Blasio AM & Spada A 2000 Calcium-sensing receptor expression and signalling in human parathyroid adenomas and primary hyperplasia. *Clinical Endocrinology* **52** 339-348.

Corbetta S, Lania A, Filopanti M, Vicentini L, Ballaré E & Spada A 2002 Mitogen-activated protein kinase cascade in human normal and tumoral parathyroid cells. *Journal of Clinical Endocrinology and Metabolism* **87** 2201-2205.

Corbetta S, Eller-Vainicher C, Filopanti M, Saeli P, Vezzoli G, Arcidiacono T, Loli P, Syren ML, Soldati L, Beck-Peccoz P *et al.* 2006 R990G polymorphism of the calcium-sensing receptor and renal calcium excretion in patients with primary hyperparathyroidism. *European Journal of Endocrinology* **155** 687-692.

Frank-Raue K, Leidig-Bruckner G, Haag C, Schulze E, Lorenz A, Schmitz-Winnenthal H & Raue F 2011 Inactivating calcium-sensing receptor mutations in patients with primary hyperparathyroidism. *Clinical Endocrinology* **75** 50-55.

Guarnieri V, Canaff L, Yun FH, Scillitani A, Battista C, Muscarella LA, Wong BY, Notarangelo A, D'Agruma L, Sacco M, *et al*. 2010 Calcium-sensing receptor (CASR) mutations in hypercalcemic states: studies from a single endocrine clinic over three years. *Journal of Clinical Endocrinology and Metabolism* **95** 1819-1829.

560 Haven CJ, Van Puijenbroek M, Karperien M, Fleuren GJ & Morreau H 2004 Differential
561 expression of the calcium sensing receptor and combined loss of chromosomes 1q and 11q in
562 parathyroid carcinoma. *The Journal of Pathology* **202** 86-94.
563
564 Huang Y & Breitwieser GE 2007 Rescue of calcium-sensing receptor mutants by allosteric
565 modulators reveals a conformational checkpoint in receptor biogenesis. *The Journal of Biological*
566 *Chemistry* **282** 9517-9525.
567
568 Hjalm G, MacLeod RJ, Kifor O, Chattopadhyay N & Brown EM 2001 Filamin-A binds to the
569 carboxyl-terminal tail of the calcium-sensing receptor, an interaction that participates in CaR-
570 mediated activation of mitogen-activated protein kinase. *The Journal of Biological Chemistry* **276**
571 34880-34887.
572
573 Kawata T, Imanishi Y, Kobayashi K, Onoda N, Okuno S, Takemoto Y, Komo T, Tahara H, Wada
574 M, Nagano N, *et al.* 2006 Direct in vitro evidence of the suppressive effect of cinacalcet HCl on
575 parathyroid hormone secretion in human parathyroid cells with pathologically reduced calcium-
576 sensing receptor levels. *Journal of Bone and Mineral Metabolism* **24** 300-306.
577
578 Lania A, Mantovani G, Ferrero S, Pellegrini C, Bondioni S, Peverelli E, Braidotti P, Locatelli M,
579 Zavanone ML, Ferrante E, *et al.* 2004 Proliferation of transformed somatotroph cells related to low
580 or absent expression of protein kinase A regulatory subunit 1A protein. *Cancer Research* **64** 9193-
581 9198.
582

583 Latus J, Lehmann R, Roesel M, Fritz P, Braun N, Ulmer C, Steurer W, Biegger D, Ott G, Dippon J,
584 *et al*. 2013 Involvement of α-klotho, fibroblast growth factor-, vitamin D- and calcium-sensing
585 receptor in 53 patients with primary hyperparathyroidism. *Endocrine* **44** 255-263.
586
587 Lian G, Lu J, Hu J, Zhang J, Cross SH, Ferland RJ & Sheen VL 2012 Filamin A regulates neural
588 progenitor proliferation and cortical size through Wee-1-dependent Cdk1 phosphorylation. *The*
589 *Journal of Neuroscience* **32** 7672-7684.
590
591 Marcocci C, Brandi ML, Scillitani A, Corbetta S, Faggiano A, Gianotti L, Migliaccio S & Minisola
592 S 2015 Italian Society of Endocrinology Consensus Statement: definition, evaluation and
593 management of patients with mild primary hyperparathyroidism. *Journal of Endocrinological*
594 *Investigation* **38** 577-593.
595
596 Martin-Salvago M, Villar-Rodriguez JL, Palma-Alvarez A, Beato-Moreno A & Galera-Davidson H
597 2003 Decreased expression of calcium receptor in parathyroid tissue in patients with
598 hyperparathyroidism secondary to chronic renal failure. *Endocrine Pathology* **14** 61-70.
599
600 Miedlich SU, Gama L, Seuwen K, Wolf RM & Breitwieser GE 2004 Homology modeling of the
601 transmembrane domain of the human calcium sensing receptor and localization of an allosteric
602 binding site. *The Journal of Biological Chemistry* **279** 7254-7263.
603
604 Mingione A, Verdelli C, Terranegra A, Soldati L & Corbetta S 2015 Molecular and clinical aspects
605 of the target therapy with the calcimimetic cinacalcet in the treatment of parathyroid tumors.
606 *Current Cancer Drug Targets* **15** 563-574.
607

Peverelli E, Mantovani G, Vitali E, Elli FM, Olgiati L, Ferrero S, Laws ER, Della Mina P, Villa A, Beck-Peccoz P, *et al.* 2012 Filamin-A is essential for dopamine d2 receptor expression and signaling in tumorous lactotrophs. *Journal of Clinical Endocrinology Metabolism* **97** 967-977.

Savoy RM & Ghosh PM 2013 The dual role of filamin A in cancer: can't live with (too much of) it, can't live without it. *Endocrine Related Cancer* **20** R341-R356.

Savoy RM, Chen L, Siddiqui S, Melgoza FU, Durbin-Johnson B, Drake C, Jathal MK, Bose S, Steele TM, Mooso BA, *et al*. 2015 Transcription of Nrdp1 by the androgen receptor is regulated by nuclear filamin A in prostate cancer. Endocrine Related Cancer **22** 369-386.

Scillitani A, Guarnieri V, De Geronimo S, Muscarella LA, Battista C, D'Agruma L, Bertoldo F, Florio C, Minisola S, Hendy GN, *et al*. 2004 Blood ionized calcium is associated with clustered polymorphisms in the carboxyl-terminal tail of the calcium sensing receptor. *Journal of Clinical Endocrinology and Metabolism* **89** 5634-5638.

Stossel TP, Condeelis J, Cooley L, Hartwig JH, Noegel A, Schleicher M & Shapiro SS 2001 Filamins as integrators of cell mechanics and signaling. *Nature Reviews. Molecular Cell Biology* **2** 138-145.

Terranegra A, Ferraretto A, Dogliotti E, Scarpellini M, Corbetta S, Barbieri AM, Spada A, Arcidiacono T, Rainone F, Aloia A, *et al.* 2010 Calcimimetic R-568 effects on activity of R990G polymorphism of calcium-sensing receptor. *Journal of Molecular Endocrinology* **45** 245-256.

632 Varshney S, Bhadada SK, Saikia UN, Sachdeva N, Behera A, Arya AK, Sharma S, Bhansali A,
633 Mithal A & Rao SD 2013a Simultaneous expression analysis of vitamin D receptor, calcium-
634 sensing receptor, cyclin D1, and PTH in symptomatic primary hyperparathyroidism in Asian
635 Indians. *European Journal of Endocrinology* **169** 109-116.
636
637 Varshney S, Bhadada SK, Sachdeva N, Arya, AK, Saikia UN, Behera A & Rao SD 2013b
638 Methylation status of the CpG islands in vitamin D and calcium-sensing receptor gene promoters
639 does not explain the reduced gene expressions in parathyroid adenomas. *Journal of Clinical*
640 *Endocrinology and Metabolism* **98** E1631-1635.
641
642 Vezzoli G, Tanini A, Ferrucci L, Soldati L, Bianchin C, Franceschelli F, Malentacchi C, Porfirio B,
643 Adamo D, Terranegra A, *et al*. 2002 Influence of calcium-sensing receptor gene on urinary calcium
644 excretion in stone-forming patients. *Journal of the American Society of Nephrology* **13** 2517-2523.
645
646 Vezzoli G, Scillitani A, Corbetta, S, Terranegra A, Dogliotti E, Guarnieri V, Arcidiacono T,
647 Macrina L, Mingione A, Brasacchio C, *et al*. 2015 Risk of nephrolithiasis in primary
648 hyperparathyroidism is associated with two polymorphisms of the calcium-sensing receptor gene.
649 *Journal of Nephrology* **28** 67-72.
650
651 Wittenveen JE, Hamdy NA, Dekkers OM, Kievit J, van Wezel T, The BT, Romijn JA & Morreau H
652 2011 Downregulation of CASR expression and global loss of parafibromin staining are strong
653 negative determinants of prognosis in parathyroid carcinoma. *Modern Pathology* **24** 688-697.
654

655 Yano S, Sugimoto T, Tsukamoto T, Chihara K, Kobayashi A, Kitazawa S, Maeda S & Kitazawa R
656 2003 Decrease in vitamin D receptor and calcium-sensing receptor in highly proliferative
657 parathyroid adenomas. *European Journal of Endocrinology* **148** 403-411.
658
659 Zhang M & Breitwieser GE 2005 High affinity interaction with Filamin A protects against calcium-
660 sensing receptor degradation. *The Journal of Biological Chemistry* **280** 11140-11146.
661

Legends

Figure 1. Filamin A protein expression in human normal parathyroid glands and parathyroid tumors. A) Representative tissue sections analyzed by immunohistochemistry with specific anti-full-length FLNA antibody. **a**, intense staining in the cytoplasm and at membrane level in epithelial cells of normal parathyroid gland; *white arrow* indicates endothelial cells, considered as positive internal control; *insert*, magnification showing membrane and cytoplasmic specific staining for FLNA in a parathyroid cells (*white head of arrow*). **b**, proportion of FLNA-expressing cells (50%) similar to normal glands in a sporadic PAds; *insert*, magnification showing FLNA-expressing cells (*white head of arrow*) besides negative or poor-expressing cells; *white arrow* indicates positivie endothelial cells. **c**, PAd section where FLNA staining involves only endothelial cells (*white arrow*). **d**, PCa section negative for FLNA specific immunostaining; *white arrow* indicates positivie endothelial cells. Scale bars represent 100 μm; a, b, c, and d, were imaged at 20X magnification; inserts were imaged at 40X magnification. **B)** Proportions of full-length FLNA-expressing cells detected by immunohistochemistry in normal parathyroid glands (PaNs), in parathyroid adenomas (PAds) and in parathyroid carcinomas (PCas); medians and interquartile ranges are shown. **C)** Confocal microscope immunofluorescent images of PAds-derived cultured single cells: **a**, Hoechst nuclear staining; **b**, FLNA-expressing (green) cells at membrane and cytoplasmic levels; **c**, CASR-expressing (red) cells; **d**, merged image showing that a small subset of cells co-expressing FLNA and CASR at high levels; *inserts*, magnification of the cell indicated by the white arrows. Scale bars represent 20 μm; a, b, c and d were imaged at 100X magnification; inserts were imaged at 200X magnification. **D)** Immunoblot with a specific antibody against the 100 kDa calpain cleaved FLNA fragment (C-FLNA) on fractioned proteins from HEK293 cells and PAds; the antibody detects also faint bands of 270 kDa in the nuclear protein fractions corresponding to the full-length FLNA (F-FLNA);

histone H3 is used as control for the nuclear proteins; C, cytoplasmic; N, nuclear; HEK293, HEK293 cell preparation; PAd, parathyroid adenoma.

Figure 2. Effects of FLNA silencing in CASR-transfected HEK293 cells. Mean expression levels quantified by densitometry of the indicated proteins in every cell preparations (left diagrams); representative western blot of the experiments (on the right). **A)** Endogenous FLNA silencing was efficient in HEK293 cells co-transfected with the empty vector, the 990R-CASR and the 990G-CASR; the representative western blot shows the full-length FLNA protein of 280 kDa; GAPDH was used as internal control; **B)** Endogenous FLNA silencing induced a down-regulation of both 990R-CASR and 990G-CASR proteins in total protein extractions, while the FLNA control siRNA did not affect the CASR expression levels; the representative western blot shows the CASR monomeric isoforms of 140-160 kDa; β-actin was used as internal control; **C)** Endogenous FLNA silencing induced a down-regulation of both 990R-CASR and 990G-CASR proteins in membrane protein fractions, while the FLNA control siRNA did not affect the CASR expression levels; the representative western blot shows the CASR monomeric isoforms of 140-160 kDa; Na/K-ATPase was used as internal control;. *, $P<0.001$; **, $P<0.05$; Ctrl siRNA, control FLNA siRNA.

Figure 3. *FLNA* and *CASR* mRNA levels in CASR-transfected HEK-293 cells and sporadic parathyroid adenomas. A) Effect of FLNA silencing on CASR mRNA expression levels in 990R-CASR-HEK293 and 990G-CASR-HEK293 cells; columns represent means and SEMs; *, $P<0.05$. **B)** Tumor *FLNA* expression levels positively correlated with *CASR* expression levels in a series of 74 sporadic parathyroid adenomas; the best-fit line (continuous line) and 95% confidence bands (dashed lines) are shown. **C)** Boxes and

whiskers representing expression levels of *FLNA* in tumors harboring the 990R allele (990R-CASR) compared with those detected in tumors harboring the 990G allele of the *CASR* gene (990G-CASR); horizontal line in the boxes represent the median values, whiskers represent minimum to maximum values, black dots represent single samples. **D)** Boxes and whiskers representing expression levels of *CASR* in tumors harboring the 990R allele (990R-CASR) compared with those detected in tumors harboring the 990G allele of the *CASR* gene (990G-CASR); horizontal line in the boxes represented the median values, whiskers represented minimum to maximum values, black dots represent single sample.

Figure 4. FLNA and CASR expression by western blot analysis in parathyroid adenomas. A) The three different bands corresponding to the monomeric immature glycosylated (140 kDa), the mature glycosylated (160 kDa) and the dimeric (280 kDa) forms of CASR were visualized; the band at 270 kDa corresponding to full-lenght FLNA was detected; actin was used as internal control; C^+, HEK293 stably transfected with CASR; C^-, HEK293 cells; K, human normal kidney; PAd, parathyroid adenoma; **B)** Lack of correlation between CASR and FLNA protein expression levels detected by western blot in parathyroid adenomas. The band intensities, corresponding to the levels of protein expression, were measured by Image J software.

Figure 5. Effect of FLNA silencing in CASR-activated ERK signaling in CASR-transfected HEK293 cells. A) In HEK293 cells transfected with the 990G-CASR and endogenous FLNA (*black dashed line*), 990G-CASR activation by increasing $[Ca^{2+}]_o$ stimulated ERK phosphorylation at higher levels than that observed in 990R-CASR-expressing cells (*black continuous line*), reaching the statistical significance at 5.0 mM

$[Ca^{2+}]_o$. Loss of FLNA by treatment with siRNA reduced 990G-CASR-induced phospho-ERK levels (*grey dashed line*) with a significant difference at 5.0 mM $[Ca^{2+}]_o$. §§, Ctrl siRNA+990G-CASR *vs* Ctrl siRNA+990R-CASR, P=0.02; §, Ctrl siRNA+990G-CASR *vs* FLNA siRNA+990G-CASR, P=0.04; *, Ctrl siRNA+990R-CASR *vs* FLNA siRNA+990R-CASR, P=0.02. **B)** Treatment of 990G-CASR-expressing HEK293 cells with increasing $[Ca^{2+}]_o$ concentrations in presence of 0.01 μM R568 overrode the FLNA loss as observed in 990R-CASR-expressing cells (*grey continuous line*), though, in presence of FLNA, 990G-CASR-expressing cells (*black dashed line*) showed higher $[Ca^{2+}]_o$-induced phospho-ERK levels than 990R-CASR-expressing cells (*black continuous line*) reaching statistically significance at 5.0 mM $[Ca^{2+}]_o$. p44/42 ERK phosphorylation levels are reported on logarithmic scale; *, Ctrl siRNA+990G-CASR *vs* Ctrl siRNA+990R-CASR, P=0.02.

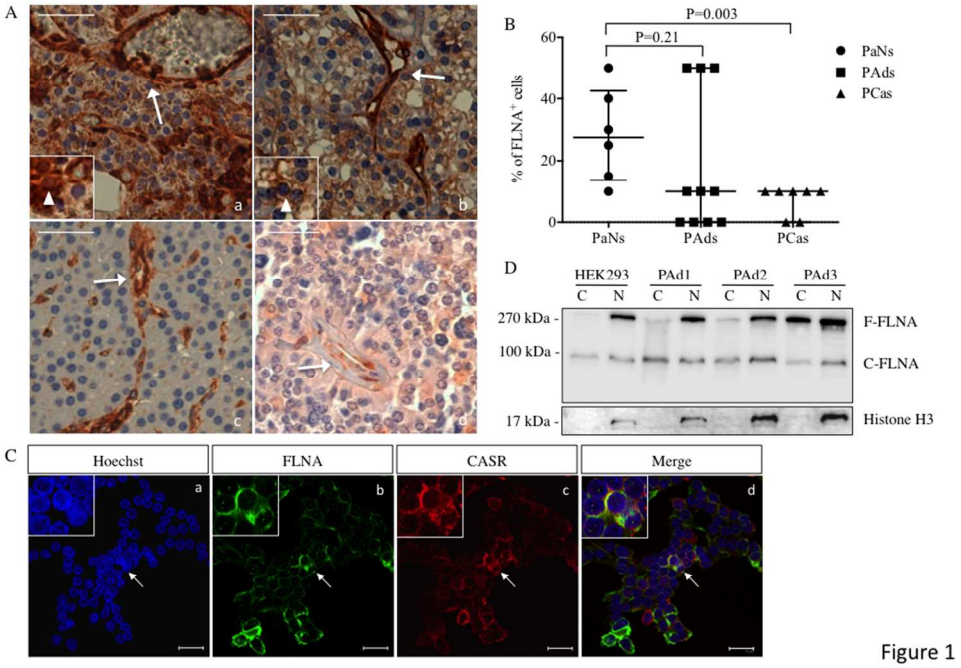

Figure 1

382x264mm (72 x 72 DPI)

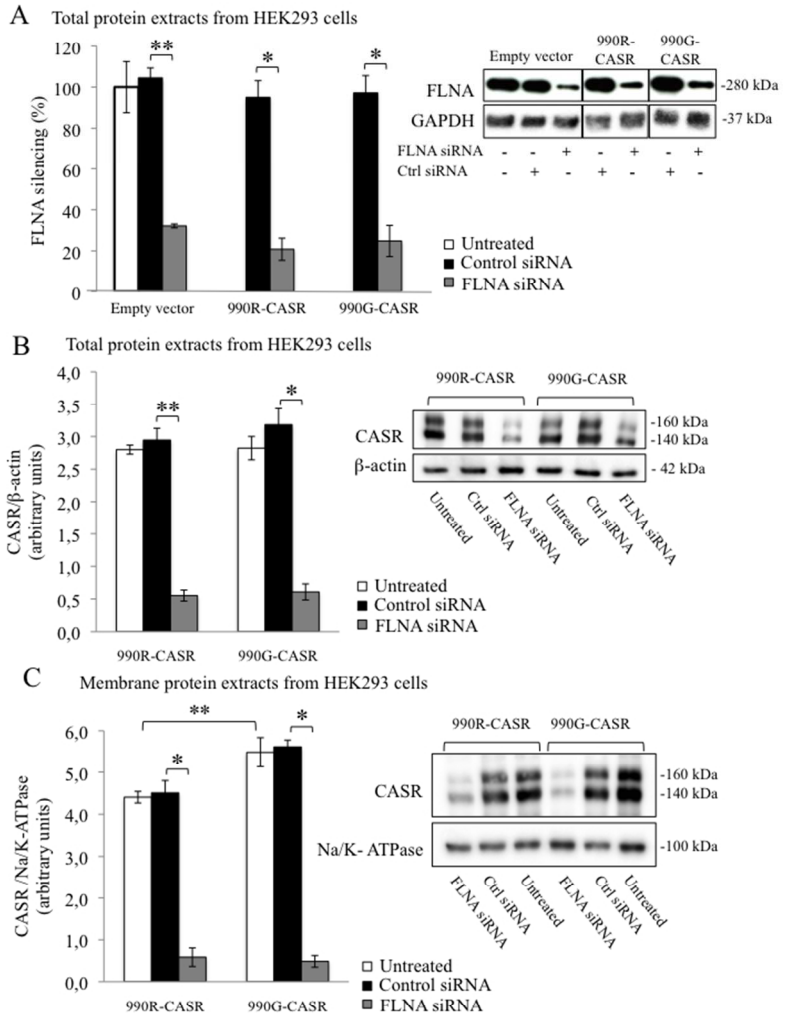

Figure 2

264x382mm (72 x 72 DPI)

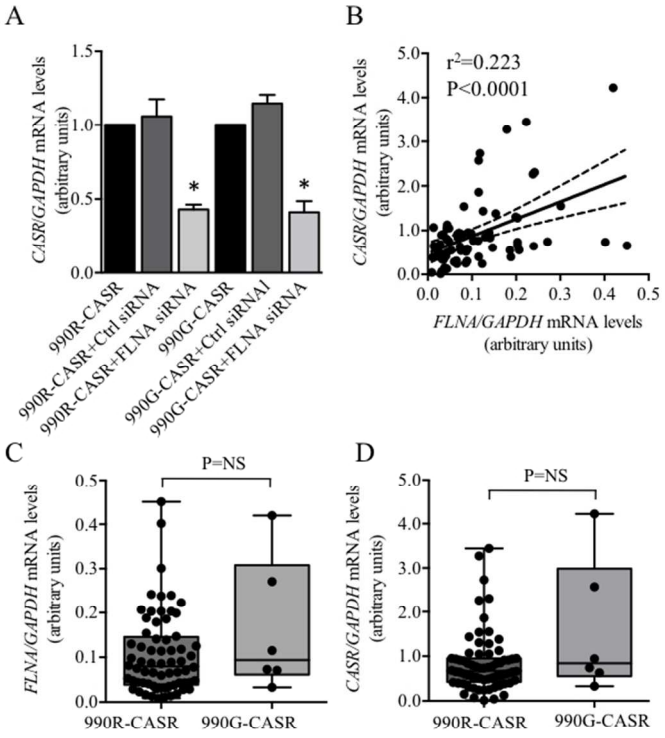

Figure 3

264x382mm (72 x 72 DPI)

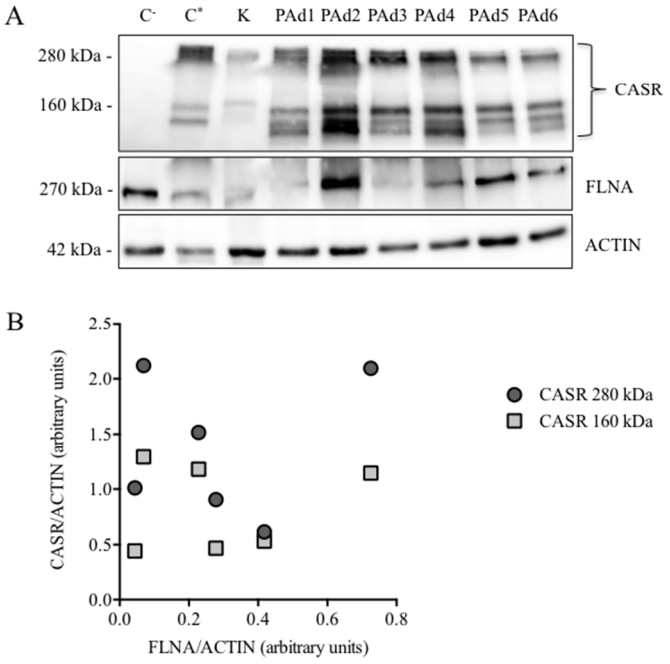

Figure 4

264x382mm (72 x 72 DPI)

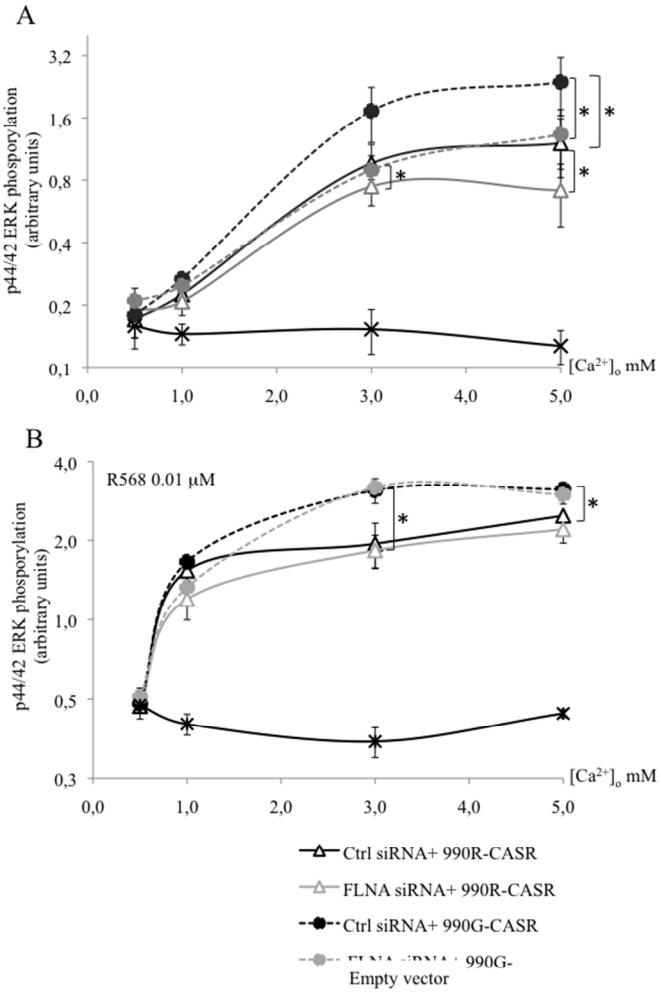

Figure 5

264x382mm (72 x 72 DPI)

Table 1. Comparisons of biochemical parameters and tumor gene expressions between severe and mild PHPT patients.

	Severe	Mild
No. patients	52	22
Serum ionized calcium (mmol/l) a	1.57 (1.47-1.67)	1.46 (1.36-1.53)
Serum alb-corr calcium (mg/dl) b	11.6 (11.0-12.3)	10.9 (10.7-11.2)
Serum iPTH (pg/ml)	201.5 (130.0-319.0)	125.0 (104.0-254.4)
Serum phosphate (mg/dl)	2.25 (1.88-2.6)	2.40 (2.13-2.73)
Kidney stones (%)	41.7	0
Osteoporosis (%)	70.8	0
Mean Qty *FLNA*	0.07 (0.04-0.19)	0.08 (0.04-0.12)
Mean Qty *CASR*	0.74 (0.41-1.08)	0.84 (0.48-1.46)

alb-corr, albumin-corrected calcium (normal value: 8.2-10.4 mg/dl); iPTH, intact parathormone, Qty, gene expression relative quantity; *FLNA*, filamin A; *CASR*, calcium sensing receptor. a, P=0.0046; b, P=0.0003. Criteria for PHPT severity are according Marcocci *et al.* 2015.